

Paraboloid electronic eye cameras using deformable arrays of photodetectors in hexagonal mesh layouts

Inhwa Jung,¹ Gunchul Shin,² Viktor Malyarchuk,¹ Jeong Sook Ha,^{2,a)} and John A. Rogers^{1,b)}

¹Department of Materials Science and Engineering, Frederick Seitz Materials Research Laboratory and Beckman Institute for Advanced Science and Technology, University of Illinois at Urbana-Champaign, Urbana, Illinois 61801, USA

²Department of Chemical and Biological Engineering, Korea University, Seoul 136-701, Republic of Korea

(Received 10 November 2009; accepted 12 December 2009; published online 15 January 2010)

We report on a type of digital camera that uses a hexagonal array of silicon photodetectors on a substrate whose surface has parabolic curvature. This elliptical paraboloid shape closely matches the image surface formed by a simple, planoconvex lens. The hexagonal arrangement provides high area coverage with an approximately circular peripheral view. Details of the design strategies and underlying features of the mechanics and optics are described. Full imaging with these parabolic cameras and comparison to planar layouts reveals improved uniformity of illumination and focus across a wide field of view. © 2010 American Institute of Physics. [doi:10.1063/1.3290244]

Digital imagers built on curved surfaces can provide additional design flexibility and, in certain cases of practical interest, improved performance, compared to those that use conventional, planar layouts.^{1–5} Historically, such planar designs have been the only option, due to deposition and fabrication methods that operate effectively only on flat, two-dimensional surfaces. Advances in stretchable electronics provide practical routes to the integration of planar device technologies onto three-dimensional, curvilinear surfaces, for functional systems with interesting characteristics;^{6–9} other approaches are also being explored for this purpose.^{10–14} Recent work using stretchable methods achieved arrays of interconnected photodetectors on hemispherical surfaces for cameras with the overall geometrical layout of the mammalian eye.⁶ Imaging results showed improved field of view and illumination uniformity and with reduced aberrations compared to planar systems when simple imaging optics were used. Simple imaging optics reduces the size and weight, and cost, of the overall system, thereby offering important advantages for devices that operate in the infrared or mount on missiles or satellites, as examples. Although this hemispherical shape is attractive, it does not represent an ideal layout, from the standpoint of the optics. For example, with a planoconvex lens, the shape of the image surface (i.e., the Petzval surface) is curvilinear with a shape that is more accurately approximated by a paraboloid than a hemisphere.⁶ Also, to cover the maximum useful area on either type of surface, a circular layout of photodetectors, rather than a rectangular arrangement, is preferred. The work reported here presents designs that use hexagonal tilings of photodetectors conformally wrapped onto paraboloid surfaces. Mechanics, optics, and device strategies to achieve such a system are described. Images collected with the resulting paraboloid cameras reveal the underlying optical effects.

The overall fabrication strategy used process flows conceptually similar to those described in detail elsewhere.^{6,7} For the work presented here, hexagonal arrays of silicon pho-

todetectors were fabricated in mechanically compressible designs using planar procedures on silicon carrier wafers, and then were conformally wrapped onto rigid, paraboloid surfaces using elastomeric transfer elements. Figure 1(a) illustrates the photodetector arrays and an additional layer for interconnect. The top silicon layer of a silicon-on-insulator wafer (1.2 μm thick Si on 700 nm SiO₂, from Soitec) provided the source material for the active elements. As shown in the figure, a unit cell consists of a silicon photodiode for light detection and a silicon blocking diode for facilitating passive matrix readout. This silicon was heavily n-doped (P506, Filmtronics) and p-doped (B219, Filmtronics) in an appropriately patterned configuration using a spin-on dopant to form this array of back-to-back diodes. Each photodetec-

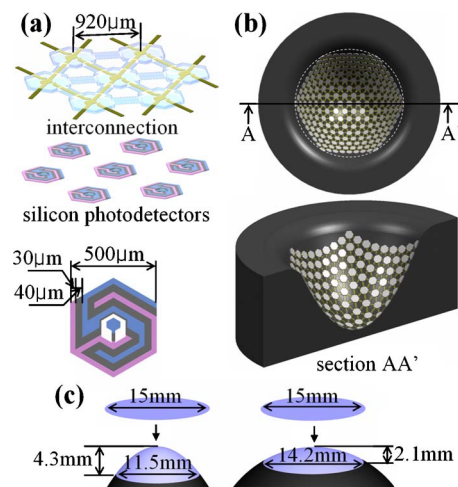


FIG. 1. (Color online) (a) Schematic illustration of a hexagonal tiling of hexagonal islands that support silicon photodetectors and blocking diodes, with interconnecting ribbons of metal (Au/Cr) encapsulated by polyimide (top), and detailed layout of an individual element, which combines a photodiode and a blocking diode (bottom). The outer, inner and middle shaded regions correspond to *p*- and *n*-doped and undoped silicon, respectively. (b) Schematic illustrations with top- and side-views of such an array conformally wrapped onto a paraboloid surface. The dotted white circle in the top frame indicates an approximately circular field of view, made possible by the hexagonal tiling. (c) Illustration for transferring a circular element (15 mm in diameter) on a parabolic surface (left), and a hemispherical surface (right).

^{a)} Author to whom correspondence should be addressed. Electronic mail: jeongsha@korea.ac.kr.

^{b)} Electronic mail: jrogers@uiuc.edu.

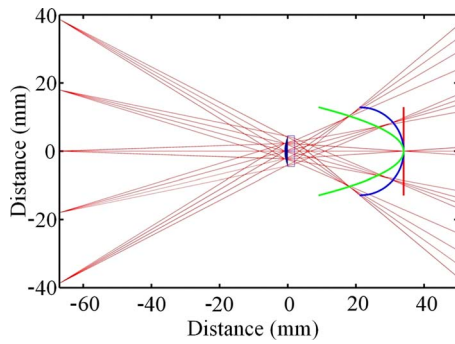


FIG. 2. (Color online) Ray tracing results to map the image surface formed by a planoconvex lens. Rays originating from five points on an object plane (left) pass through the lens (center) and cross at points that define an image surface (right). The actual image surface is well described by a paraboloid of revolution (left solid line). The middle and right solid lines correspond to approximations based on hemispherical and planar surfaces, respectively.

tor was interconnected by narrow metal lines [Cr (5 nm)/Au (150 nm)] encapsulated with polyimide ($\sim 1 \mu\text{m}$, Sigma Aldrich) on top and bottom. This structure places the metal at the neutral mechanical plane, thereby providing significantly higher levels of bendability and robustness compared to silicon or metal alone. Such enhanced bendability is critically important for the planar to paraboloid geometry transformation, described next, due to the large strains that must be accommodated, compared to the hemispherical case.⁶

For transformation, a thin membrane of poly(dimethylsiloxane) (PDMS; Dow Corning) with the shape of a paraboloid was first stretched in a radial manner until approximately flat, using a custom mechanical stage. Next, the prefabricated, planar hexagonal photodetector array was transferred to the PDMS. Releasing the radial tension, caused the PDMS to return to its original paraboloid shape, carrying the array with it. In this process, the narrow, polymer/metal/polymer interconnect lines delaminated from the PDMS to form arc-shaped structures that effectively accommodated the associated compressive strains. The array was then transferred and bonded to a paraboloid substrate using a thin coating of an optical adhesive (NOA 703, Norland). Further details of the transfer method appear elsewhere.^{6,7} Figure 1(b) provides top- and side-view schematic illustrations of a resulting array. Compared to a square arrangement, the hexagonal tiling more effectively fills the circled area, and at the same time follows the parabolic curvature (top figure). The sliced view of the transferred array (bottom figure) shows the curvature of a parabolic surface, $y = 1/(4f)r^2$, where f is a distance parameter related to the diameter and numerical aperture of the imaging lens. We obtained this value empirically by fitting the results of ray tracing modeling described, in detail, next. Working cameras were completed by mounting in a printed circuit board (PCB), establishing electrical interconnects from the edge of the array using silver conductive epoxy (Chemtronics) and connecting to a computer for image acquisition.

To determine the specific shape of the paraboloid substrate, we used ray tracing analysis (Optical Bench)^{3,15,16} to define the image surface. Figure 2 shows the imaging lens that was used, and a set of representative calculated rays. Fans of rays originating at the object plane (-67 mm) were projected through the planoconvex imaging lens. The location of best focus at the center of the image (34 mm) was determined, and flat, hemispherical, and parabolic surfaces

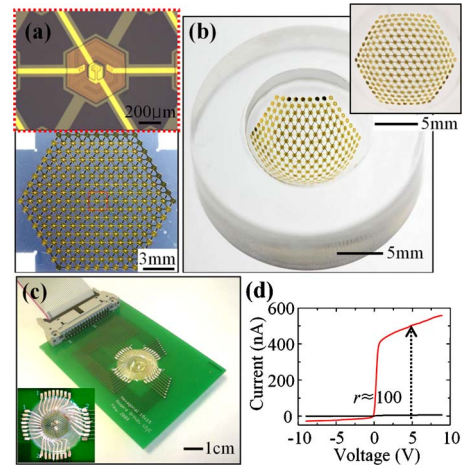


FIG. 3. (Color online) (a) Photograph of a hexagonal photodetector/diode array on a planar surface (bottom) and optical microscope image of a single unit cell (top). (b) Photograph of such an array transferred onto a parabolic surface, where the inset provides a top view. (c) Photograph of completed imager mounted in a PCB, where the inset shows a top view of the device area. (d) Representative current-voltage response of a pixel in the camera of frame (c), with a light on (top) and off (bottom), where r is ratio of current between on/off states.

(right, middle, left solid lines in Fig. 2, respectively) were positioned accordingly. Tracking shifts in the position of best focus for rays corresponding to off-center parts of the image revealed that the curvature in this case follows a parabolic function: $y = 0.132r^2$ in millimeter scale (paraboloid of revolution, left solid line in Fig. 2). The hemispherical and flat surfaces provide moderate and poor approximations to this actual shape, respectively. These modeling results defined our choices of imaging lenses and parabolic surface shapes.

The paraboloid surface itself was fabricated from an aluminum block by a numerical control machine (EZ-Path/Bridgeport Romi) followed by polishing to produce a smooth surface. The resulting aluminum piece was replicated, using soft lithographic molding techniques, into an acrylic resin for the device substrate and into a thin membrane of PDMS for the transfer element. Figure 1(c) shows the geometry associated with transferred arrays, with comparison to the hemispherical case. The deformations required for geometry transformation in the system presented here are roughly twice as large as those reported previously for the hemispherical case (i.e., strain ranges of $\sim 25\%$ and $\sim 12\%$ for these paraboloid and hemispherical shapes, respectively). In spite of the relatively high degree of curvature, yields on working pixels in systems reported here were as high as 91%. The yields can be improved by use of dedicated manufacturing and clean room facilities.

Figure 3(a) shows the planar array, immediately after fabrication. Transfer to planar or paraboloid surfaces, followed by integration with a PCB to provide a ribbon cable interface to an external computer for image collection completed the devices. An array after transfer to a parabolic surface appears in Fig. 3(b); the inset shows a top view of the same device. Figure 3(c) shows this imager attached to a PCB and interfaced to a computer. Figure 3(d) presents representative current (I)-voltage (V) characteristics of an individual photodetector/diode element in the array. The red and black curves were measured with the light on and off, respectively. The current ratio between on/off states at 5 V was ~ 100 .

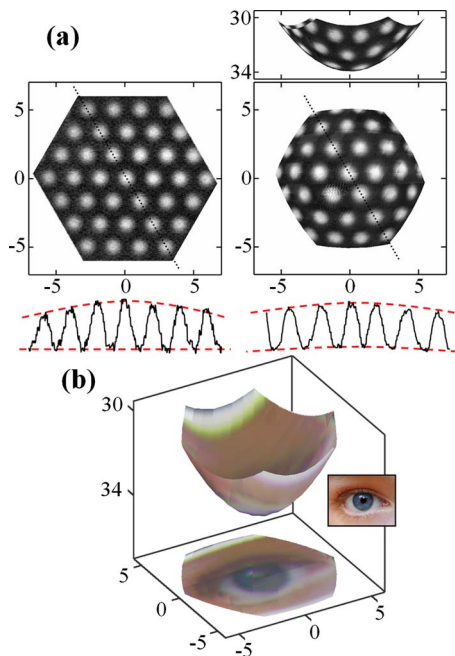


FIG. 4. (Color online) (a) Image of a test pattern consisting of a hexagonal array of white dots (2 mm in diameter and 4 mm in pitch) captured with a planar camera (left) and a paraboloid camera (upper right) and a planar projection (lower right). The bottom frames present intensity profiles collected along the dotted lines in the images. (b) Examples of reconstructed color picture collected with the paraboloid camera. The top part of this frame corresponds to the image itself, while the bottom frame provides a planar projection. The inset at the right shows the object. (The axes units are millimeters.)

A planoconvex lens (diameter of 9 mm and focal length of 22.8 mm, JML Optical Industries, Inc.) was used with the camera, Fig. 3. Imaging involved passing light through a transparent film placed in front of the device. Previously described systems for data acquisition, computer interfacing with mux/demux electronics and software control systems were used.⁶ Due to the modest number of pixels in the cameras reported here (i.e., 169), small-range scanning of the detector (for flat device) or object (for parabolic device) was used to improve the effective resolution, for the purpose of evaluating detailed aspects of the imaging capabilities. Extending to the megapixel range is likely accomplished most easily through tiled designs that incorporate many photodetectors at each island in the array.⁸ The response of each pixel was calibrated by a leveling procedure that used data collected with the camera in the dark and illuminated uniformly, without the lens in place. This procedure was straightforward for the planar array. For the paraboloid case, we included multipliers to account for the angular dependence of the power per unit area striking the surface of each photodetector, depending on its position. The angular dependence of the reflectivity can, in principle, also be important. Fresnel calculations show, however, that this effect is negligible in the range considered here (i.e., zero to roughly 60°). For image construction, we used the physical location of each pixel, as determined directly by mapping of their lateral positions locations using top view photographs of the device (EOS 1Ds Mark III, Canon), similar to that shown in Fig. 3(b). The positions in the out of plane direction were calculated based on the parabolic function that describes the surface of the substrate.

Figure 4(a) shows a test patterning consisting of a hex-

agonal array of circular white spots (4 mm in pitch and 2 mm in diameter) imaged with a parabolic and a flat camera with otherwise identical designs and procedures for image capture. Careful examination and comparison of the two images shows clearly that the planar case focuses more poorly at the periphery of the field of view, compared to the parabolic case, as expected from simple ray tracing analysis of Fig. 2. Another advantage, not apparent from Fig. 2, is that the uniformity of illumination is better in the parabolic case than the planar. This effect can be shown by extracting intensity profiles across each image. The flat camera shows a systematic variation, with lower intensities in the peripheral regions, of $\sim 25\%$. The parabolic case shows an approximately uniform distribution of intensity. Figure 4(b) provides an example of a color image collected by the paraboloid camera. [Note that in both Fig. 4(a) and 4(b), the planar projections of the images exhibit expected distortions.]

In conclusion, the work presented here demonstrates feasibility of two advanced design aspects for curved focal plane cameras—paraboloid surface shapes and hexagonal tilings of photodetectors. Actual images collected with such systems demonstrate key aspects of their operation. The associated enhancements and design flexibility could create new opportunities in digital imaging.

Inhwa Jung and Gunchul Shin contributed equally to this work. We thank T. Banks for help in processing by use of facilities at the Frederick Seitz Materials Research Laboratory. The mechanics and materials components of the work were supported by the National Science Foundation under Grant No. ECCS-0824129 and a MURI award. J.S.H. and G.S. acknowledge Korea Science and Engineering Foundation (KOSEF) through the National Research Laboratory Program funded by the Ministry of Science and Technology (Grant No. ROA-2007-000-20102-0).

- ¹L. Lee and R. Szema, *Science* **310**, 1148 (2005).
- ²S.-B. Rim, P. B. Catrysse, R. Dinyari, K. Huang, and P. Peumans, *Opt. Express* **16**, 4965 (2008).
- ³A. Walther, *The Ray and Wave Theory of Lenses* (Cambridge University Press, Cambridge, UK, 1995).
- ⁴P. Swain and D. Mark, *Proc. SPIE* **5499**, 281 (2004).
- ⁵T. Grayson, *Proc. SPIE* **4849**, 269 (2002).
- ⁶H. C. Ko, M. P. Stoykovich, J. Song, V. Malyarchuk, W. M. Choi, C.-J. Yu, J. B. Geddes III, J. Xiao, S. Wang, Y. Huang, and J. A. Rogers, *Nature (London)* **454**, 748 (2008).
- ⁷H. C. Ko, G. Shin, M. P. Stoykovich, J. W. Lee, D. H. Kim, S. Wang, J. S. Ha, Y. Huang, K. C. Hwang, and J. A. Rogers, *Small* **5**, 2703 (2009).
- ⁸G. Shin, I. Jung, V. Malyarchuk, J. Song, H. C. Ko, Y. Huang, J. S. Ha, and J. A. Rogers, "Micromechanics and Advanced Designs for Curved Photodetector Arrays in Hemispherical Electronic Eye Camers," *Small* (to be published).
- ⁹S. Wang, J. Xiao, I. Jung, J. Song, H. C. Ko, M. P. Stoykovich, Y. Huang, K. C. Hwang, and J. A. Rogers, *Appl. Phys. Lett.* **95**, 181912 (2009).
- ¹⁰H. C. Jin, J. R. Abelson, M. K. Erhardt, and R. G. Nuzzo, *J. Vac. Sci. Technol. B* **22**, 2548 (2004).
- ¹¹X. Xu, M. Davanco, X. Qi, and S. R. Forrest, *Org. Electron.* **9**, 1122 (2008).
- ¹²P. I. Hsu, R. Bhattacharya, H. Gleskova, M. Huang, Z. Xi, Z. Suo, S. Wagner, and J. C. Sturm, *Appl. Phys. Lett.* **81**, 1723 (2002).
- ¹³P. J. Hung, K. Jeong, G. L. Liu, and L. P. Lee, *Appl. Phys. Lett.* **85**, 6051 (2004).
- ¹⁴R. Dinyari, S. B. Rim, K. Huang, P. B. Catrysse, and P. Peumans, *Appl. Phys. Lett.* **92**, 091114 (2008).
- ¹⁵B. Gustavsson, *Optical_bench* (<http://www.mathworks.com/matlabcentral/fileexchange/1649>).
- ¹⁶M. Born and E. Wolf, *Principles of Optics*, 7th ed. (Cambridge University Press, New York, 1999).